Research Article

Metakaolinization Effect on the Thermal and Physiochemical Propperties of Kankara Kaolin

Nurudeen Salahudeen*
Department of Chemical and Petroleum Engineering, Bayero University, Kano

* Corresponding author. E-mail: nsalahudeen.cpe@buk.edu.ng DOI: 10.14416/j.ijast.2018.04.003
Received: 26 June 2017; Accepted: 23 November 2017; Published online: 17 April 2018

Abstract
The effect of Metakaolinization on the thermal and physiochemical propperties of Kankara kaolin is presented. Thermogravimetric Analysis (TGA) and Differential Thermogravimetric (DTG) scan of Kankara kaolin indicated that kaolin was transformed to metakaolin at temperature above 600°C. The TGA/DTG scan of the metakaolin produced showed that the material was thermally stable at temperature range of 600–900°C. The metakaolin was characterized using X-ray Diffraction (XRD), Scanning Electron Microscopy (SEM) and Brunauer-Emmett-Teller (BET) texture analysis. The metakaolin formed was amorphous, having average particle size of 2.5 µm. The specific surface area values of the raw kaolin and the metakaolin formed were 12.95 and 19.38 m^2/g respectively. The pore volume values of the raw kaolin and the metakaolin were 0.0038 and 0.0585 cm^3/g respectively.

Keywords: Kaolin, Metakaolin, Physiochemical, Thermal stability

1 Introduction

Kaolin is a planar hydrous phyllosilicate clay mineral, belonging to an interlayer structural class referred to as 1:1. Kaolin possesses a dioctahedral 1:1 (T–O) structure having structural dimension in the nanometer range; the thickness of a 1:1 (T–O) layer is about 0.7 nm [1]. Kaolin also consists of non-phyllosilicate minerals such as carbonates, feldspars and quartz, together with the (hydr)oxides of iron and aluminum, which are referred to as 'non-clay constituent' or 'accessory minerals' [1], [2]. Kaolin is one of the most abundant minerals in soils and sediments; it is a common weathering product of many tropical and sub-tropical soils [2], [3]. Kaolin has been a very useful and versatile domestic and industrial material dating back to before the industrial revolution age. The oldest known use of kaolin is as a ceramic raw material [4]. Other uses of kaolin include application in medicine, coated paper, paint, membrane formation and construction [5]. Calcination of kaolin at high temperatures transforms kaolin minerals to other phases. The transformation phases are metakaolin, spinel and mulite crystoblite; they occur at calcination temperatures of 500–850, 900–950 and ≥ 1050°C respectively [6], [7]. Metakaolin is a very reactive transformation phase of kaolin formed by calcination of kaolin; the calcination results into dehydroxylation of kaolin, which results in cleavage of the interlayer T–O bonds in the kaolin structure. The absence of strong layer–layer binding makes metakaolin very reactive. Owing to its high reactivity, metakaolin is used as absorbent and catalyst support [8]. It is used as catalyst for the alkylation of benzene with benzyl chloride [9] and for synthesis of heterogeneous solid catalyst in transesterification processes for biodiesel production [10]. It is also used for synthesis of different phases of zeolite [11]. Other uses of metakaolin

Please cite this article as: N. Salahudeen, "Metakaolinization effect on the thermal and physiochemical propperties of Kankara kaolin," *KMUTNB Int J Appl Sci Technol*, vol. 11, no. 2, pp. 127–135, Apr.–Jun. 2018.

include its varied applications in formulation of construction materials such as high performance concrete, fibre cement and ferrocement [12]–[18].

Varied conditions have been reported for production of metakaolin from kaolin. Rashad, [16] reported temperature range of 600–850°C at soaking time range of 1–12 h, depending on the chemical composition of the kaolin. However, he also reported that most of the popular works in this area reported calcinations at 650°C for 1 h, 700°C for 2 h and 750°C for 3 h as the optimum calcination conditions. Wang *et al*. [17] reported production of metakaolin at 800 and 900°C for 4 h. This work has the disadvantage of longer calcination time and higher temperature range. Wang *et al*. [19] reported production of metakaolin at temperature range of 600–900°C. This work has the advantage of studying wider range of temperature but disadvantage of longer calcination time. Chandrasekhar *et al*. [20], Rahier *et al*. [21] and Zhang *et al*. [22] prepared metakaolin by calcining kaolin at 700°C for 1 h. This work has the advantage of lower temperature and lower calcination time. Shvarzman *et al*. [23] reported that kaolin shows low level of dehydroxylation degree at temperature < 570°C. But kaolin becomes fully transformed to metakaolin at temperature range of 570–700°C. The advantage of this work is that it was able to identify the temperature metakaolinization begins. Fabbri *et al*. [24] reported 650 and 750°C as the best metakaolinization temperature and 2 h as the optimum soaking time. Ilic *et al*. [25] reported that several previous studies showed that 2 h soaking is sufficient to attain maximum dehydroxylation of kaolin at temperatures higher than 600°C. The advantage of these works [24], [25] is that they were able to report the optimum calcination time as 2 h.

The objectives of the current study are to investigate the TGA/DTG behaviour of kaolin within temperature range below 900°C so as to establish the point where metakaolinization phase transformation occurs within this temperature range; and to study the physiochemical properties of metakaolin produced in the perspective of giving an insight into its suitability for catalytic applications. This work was able to determine the kaolinite content of Kankara kaolin, the extent of dehydroxylation of the Kankara kaolin during metakaolinization and the effect of metakaolinization on the specific surface area and pore volume of Kankara kaolin.

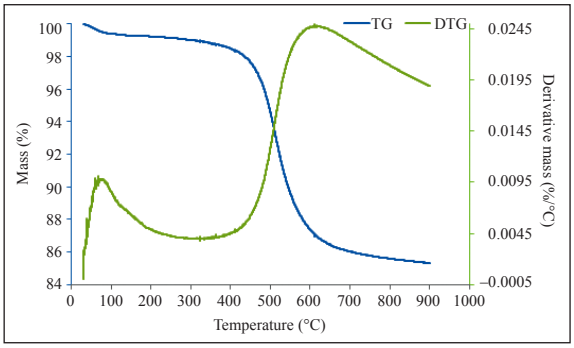

Figure 1: (Left) TGA (Right) DTG cuves of Kankara kaolin.

2 Materials and Methods

Raw kaolin was mined using representative mining from Kankara Local Government Area of Katsina State–Nigeria, the satellite map of the mining site is provided in Figure 1. The mined sample was crushed using mortar and pestle then wet beneficiated as presented in Salahudeen *et al*. [26] and Ahmed *et al*. [27]. For a batch beneficiation; X gram of the raw kaolin sample was crushed. The crushed clay was wet-beneficiated by soaking in water at 0.1 kg/L clay-to-water ratio, The soaked clay was stirred at 200 rpm for 3 h to separate all agglomerated clay particles, then the it was allowed to settle overnight The supernatant water was decanted and the clay slurry was sieved using Tyler mesh sieve of mesh size 200 (75 µm aperture opening). The weight of beneficiated kaolin collected as the filtrate was recorded as Y gram. The beneficiated kaolin was dried at 100°C for 6 h, it was ball milled and sieved to particle size less 75 µm.

The kaolinite content of the beneficiated clay was evaluated using Equation (1).

$$K = 100 - \frac{X}{Y} \times 100 \tag{1}$$

Where, K = kaolinite content (%), X = mass of the raw kaolin sample (g), Y = mass of the beneficiated kaolin (g).

Meatakaolinization of the Kankara kaolin was carried out by calcining/dehydroxylating the clay at 700°C for 2 h in a chamber furnace (Nabertherm). Equation (2) expresses the chemical equation involved in the calcination process.

$$Al_2O_3•2SiO_2•2H_2O \rightarrow Al_2O_3•2SiO_2 + 2H_2O \quad (2)$$

Thermogravimetry analysis was carried out using Perkin Elmer simultaneous thermal analyzer, STA 6000. The method used was thermal scan from 30 to 900°C at heating rate of 10°C/min and cooling at 20°C/min from 900 to 30°C. Nitrogen was used as the purge gas at flow rate of 20 mL/min. For a batch scan 20 mg sample was placed in the platinum crucible, and then placed in the TGA furnace, the equipment was conditioned for about 30 min then the thermal scan was commenced. XRD patterns were recorded from Bragg's angle (2θ of 10° to 70° using Pananalytical X'pert[3], operated at continuous scanning; scanning speed of 5°/min, generator settings of 10 mA and 40 kV, and CuKα node material. XRF analysis was carried out using Minipal 4, Pananalytical X-ray fluorescence analyzer. BET Nitrogen adsorption, specific surface area analysis was carried out using Autosorb Station1, Quantachrome. Outgassing was carried out at 300°C for 4 h and N_2 absorption/desorption at 77.350 K. SEM analysis was carried using JEOL Field Emission Scanning Electron Microscope JSM–7600F operated at vacuum of about 9.634×10^{-5} torr. TEM analysis was carried using JEOL JEM–1230 TEM operated at vacuum of about 9.634×10^{-5} torr.

3 Results and Discussions

Using Equation (1) the kaolinite content of Kankara kaolin was evaluated as 73%. Figure 2 shows the TGA/DTG curves for the Kankara kaolin at thermal scan of 30–900°C at heating rate of 10°C/min. It could be observed from the left ordinate that the total TGA mass depletion resulting from the thermal treatment was 15 wt%. The TGA mass depletion could be attributed to the mass loss due to dehydroxylation of the clay during metakaolinization process. This value was in a close proximity to the Loss on Ignition (LOI) value obtained in the chemical composition of the clay presented in Table 1. The DTG curve tells the actual temperature responsible for the thermogravimetric mass depletion [28], [29]. It could be seen from the DTG curve that the mass depletions occurred at temperatures of about 100 and 600–700°C. The loss at 100°C occurred at 0.0095 wt%/°C, as shown by the right ordinate. This could be attributed to loss of physically adsorbed water molecules within the clay pores and on the

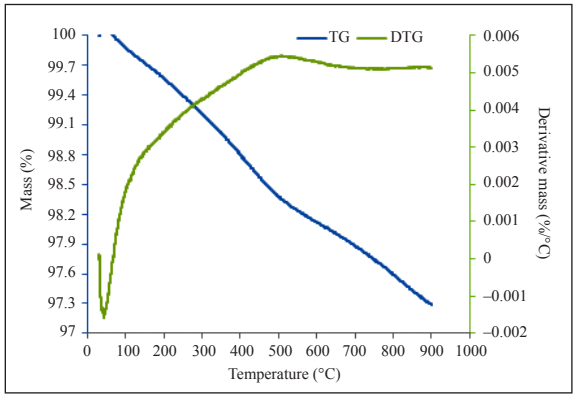

Figure 2: (Left) TGA (Right) DTG curves for metakaolin.

clay surfaces. The mass loss at 600–700°C occurred at 0.0245 wt%/°C, which was the highest thermal differential mass loss rate. The differential mass loss at 600–700°C was due to loss of chemically combined water resulting to phase transformation of the kaolinite to metakaolin. Compared to other related works, Fabbri *et al*. [24] have reported reported 500°C as the DTG point responsible for the phase transformation of the kaolin used in their work. In this investigation a minimum TGA peak was observed around 350–400°C, which afterwards rose until a maximum was attained at about 600–700°C. The minimum point could be attributed to the point where the metakaolinization phase transformation began, therefore the transformation continued until it was completed at the peak point of 600–700°C. The differential rate of the transformation at the the starting point was very low; occurring at about 0.0020 wt%/°C, whereas at the peak point the rate was much higher; occurring at 0.0245 wt%/°C.

Table 1: Chemical composition of the Kankara kaolin and metakaolin

Oxide (wt%)	Kankara Kaolin	Metakaolin
Al_2O_3	27.81	32.94
SiO_2	52.04	59.16
Na_2O	0.57	0.26
K_2O	1.89	1.82
MgO	0.50	0.46
CaO	1.19	1.33
CuO	0.02	0.01
TiO_2	0.12	0.13
Fe_2O_3	0.93	1.82
LOI	14.70	1.66

Figure 2 shows the TGA/DTG curves for the metakaolin at thermal scan of 30–900°C at heating rate of 10°C/min. It could be observed that the total mass depletion resulting from the thermal treatment was about 2.7 wt%. This was only 18% of the mas depletion recorded for the kaolin. The temperature responsible for the mass loss in the metakaolin was not vividly identified like in the DTG curves of the kaolin. However, some faint thermal peak could be observed at about 600°C. The low mass depletion observed for the metakaolin was because the material had already undergone phase transformation within the temperature range of the thermal treatment during metakaolinization, therefore, further heating within the same temperature range would not likely result into any transformation or major mass depletion in the material. It is worth noting that since the metakaolinization was carried out in bulk, it is likely that some little fraction of the material was not completely transformed, therefore the slight DTG peak and the little mass depletion observed were likely due to complete phase transformation of such unconverted fractions to the metakaolin phase. At farther temperature range (600–900°C), the metakaolin DTG profile appeared thermally stable showing that the material was not sensitive to thermal treatment at that temperature range.

Figures 3 and 4 show the XRD patterns of the Kankara kaolin and the metakaolin respectively. It could be observed that the Kankara kaolin was relatively crystalline, when compared to the XRD of the metakaolin which was highly amorphous. Considering the Kankara kaolin XRD patterns, it would be observed that the characteristic peaks of Kaolinite were present at Bragg's angles of 12.35, 19.89, 20.38, 24.88, 34.94, 35.95, 36.06, 38.35, 45.24, 54.88, and 62.37°. The peak at 26.65° was due to crystalline silica, also known as quartz [30]–[32]. The peak at 17.4° was due to mica-monimorillonite [30]. The highest kaolinite peaks were at Bragg's angles of 12.35 and 24.88°; having intensity of about 500 and 550 counts respectively, while the quartz peak had intensity of about 350 counts. Considering the XRD pattern of the metakaolin, it would be observed that the XRD pattern was highly amorphous. The crystalline structure of the raw kaolin crumbled and became amorphous metakaolin as a result of calcination effect on the raw kaolin. The quartz peak having intensity of about 380 counts was the only obvious mineral peak

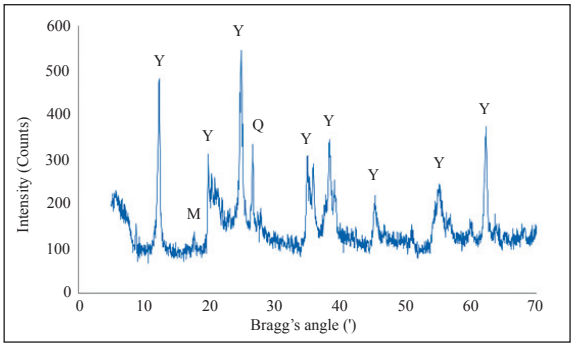

Figure 3: XRD Patterns of kankara kaolin.

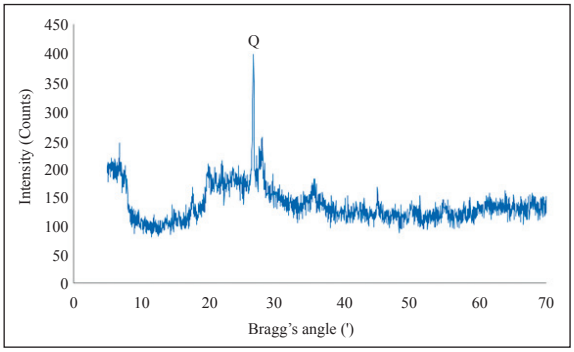

Figure 4: XRD Patterns of metakaolin produced.

observable in the XRD of the metakaolin, this was similar to the finding of Wang *et al*. [17].

This can be explained by the fact that quartz mineral which was an impurity in the raw Kankara kaolin is structurally stable at thermal treatment below 1050°C; Edomwonyi-Out *et al*. [7]. Table 1 presents the chemical composition of Kankra kaolin and the metakaolin produced. It would be observed that the LOI of the Kankara kaolin was 14.70 wt%, this concurred closely with the mass depletion of 15 wt% noted in the TGA result of kaolin as discussed earlier. It would also be noted from Table 1 that the LOI value after metakaolinization was 1.66 wt%; this was also relatively close to the 2.7 wt% mass depletion observed in the TGA result of kaolin as discussed earlier.

The decrease in LOI after metakaolinization could be attributed to high dehydroxylation of the clay during the matakaolinization process which implies dehydration of chemically combined water molecules in form of –OH group. It could be observed that the chemical composition of the Kankara kaolin was relatively similar to the kaolin used by Fabbri *et al*.

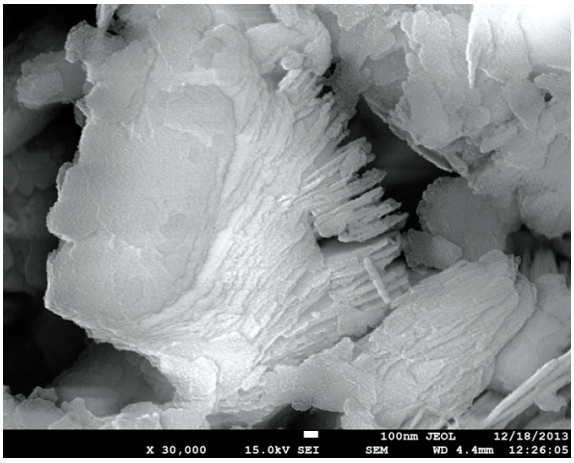

Figure 5: SEM image of Kankara kaolin.

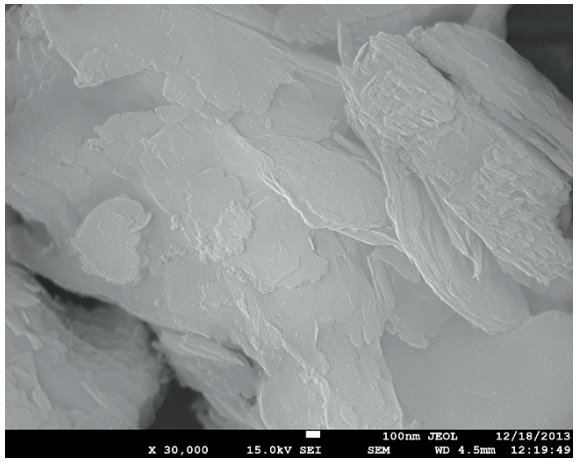

Figure 6: SEM image of metakaolin.

[24] except that the Si/Al of the Kankara kaolin was relatively higher, having value of 1.87, while those reported by Fabbri *et al*. [24] were in the range of 1.16–1.27. Table 2 shows comparison of the chemical composition of Kankara kaolin with Elefun kaolin in Nigeria and other kaolin from other countries [33]–[35]. It could be observed that Kankara kaolin has reasonably low impurity such as Fe_2O_3 and TiO_2. It could also be observed that Kankara kaolin has relatively high Si/Al ratio of 1.90 which is comparable to that of the Egyptian kaolin and the German kaolin, whereas the Elefun and USA kaolin have low Si/Al ratio of about 1.30.

Figure 5 shows the SEM image of Kankara kaolin, the platelet structure of kaolinite clay which normally portrays booklet morphology as reported in the literature [1], [36]–[41] could be clearly observed. The micrograph shows booklet morphology consisting of platelet sheets of kaolinite mineral. The average particle size was estimated as 1.0 μm. Figure 6 shows the SEM image of the metakaolin, it could be noticed that the booklet morphology observed in the micrograph of the kaolin has been lost in the morphology of the metakaolin. Unlike the kaolinite morphology, the morphology of the metakaolin was largely lump-like, although little platelet morphology could also be observed. The lump-like morphology of the metakaolin could be attributed to the highly amorphous nature of the material resulting from crumbling of the kaolinite structure, as was already identified by the analysis of the XRD results earlier discussed. The few platelet

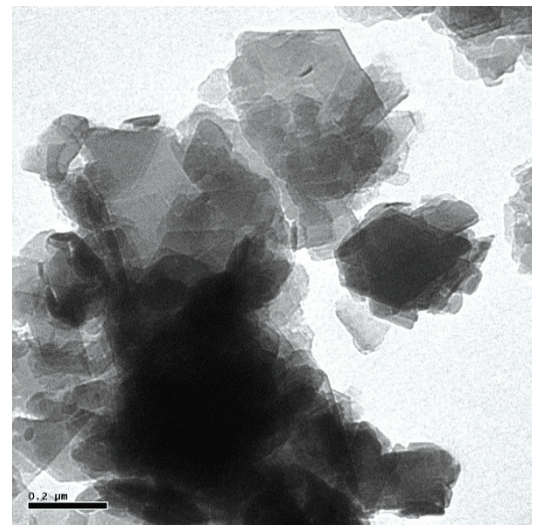

Figure 7: TEM image of Kankara kaolin.

morphology observed in the material was as a result of the crystalline silica present in the metakaolin as the XRD results have earlier shown. The average particle size of the metakaolin was estimated as 2.5 μm.

Figure 7 shows the TEM image of the Kankara kaolin. The TEM image revealed the definite shape of a unit clay particle. Different authors have commented on the diverse size and shape of kaolin particles [42], [43]. It has been reported that natural kaolin is often associated with high-defect structures. However, as revealed in Figure 7 the Kankara kaolin possessed tetrahedral and hexagonal, euhedral morphology.

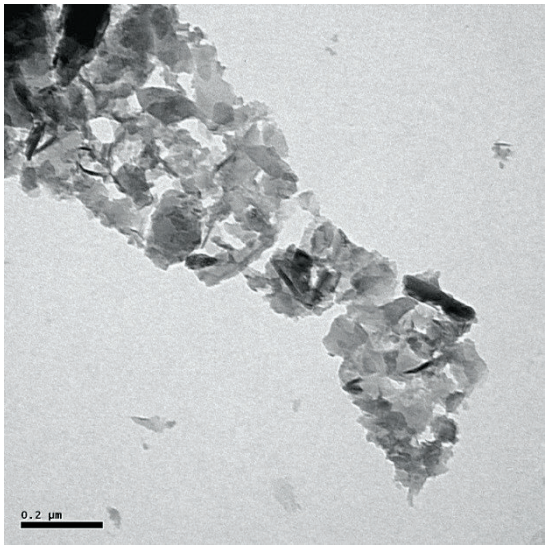

Figure 8: TEM image of metakaolin.

Although some of the clay particles were overlapping in the TEM image, the average unit crystal size of the Kankara kaolin was estimated as 350 nm. Figure 8 shows the TEM images of the metakaolin, the particle structure portrayed a hollow anhedral morphology showing irregular particle shapes. The irregularity of the particles showed that the material was highly amorphous, this observation concurs with the XRD result discussed earlier. The structural shape irregularity could be as a result of the structural crumbling of the initial kaolinite structure experienced during the metakaolinization process, as was already shown by the XRD and the SEM analyses. The average unit crystal size of the metakaolin was estimated as 150 nm.

Table 2 presents the BET results for Kankara kaolin and the metakaolin produced. The kaolin had a low specific surface area value of 12.95 m^2/g and pore volume of 0.0038 cm^3/g. The specific surface area of the clay increased by 49.7% after metakaolinization. This observation was similar to the finding of Fabbri *et al*. [24], where the specific surface area of the kaolin used increased by 52%, when calcined at 650°C for 2 h. The pore volume of Kankara kaolin increased exponentially by 1,439% after metakaolinization. The increase in the specific surface area could be attributed to loss of the initial crystallinity of the kaolinite mineral as was already shown by the XRD results. The crumbling of the ordered platelet structure of kaolinite due to calcination effect had resulted into a higher specific surface area, higher pore volume and more amorphous structured metakaolin. The increase in the specific surface area and pore volume were likely the reason why metakaolin has been reported to be very reactive [10].

Table 2: BET specific surface area and pore volume for Kankara kaolin and metakaolin

Sample	Specific Surface Area (m^2/g)	Pore Volume (cm^3/g)
Kankara Kaolin	12.95	0.0038
Metakaolin	19.38	0.0585

4 Conclusions

TGA/DTG analysis carried out has shown that kaolin is thermally stable below 600°C. This investigation showed that kaolin transformed to metakaolin at calcination temperature range of 600–700°C. TGA/DTG analysis of the metakaolin formed showed that matakaolin is thermally stable at temperature range of 600–900°C. The XRD, SEM and TEM characterizations carried out showed that; metakaolin was highly amorphous; the only crystalline peak present in its crystallographic pattern was due to the presence of quartz. The average particle size of metakaolin formed was 2.5 µm. The process of transformation of kaolin to metakaolin resulted into increase in the specific surface area and pore volume of kaolin by 49.7% and 1,439% respectively. These increases were likely the reasons why metakaolin has been reported to be very reactive [10]. The metakaolin produced is recommended for use as catalyst support, due its improved specific surface area and pore volume, and due to its thermal stability, which can be of additional advantage in elevated temperature catalytic applications.

Acknowledgements

The authors gratefully acknowledge Petroleum Technology Development Fund (PTDF) Abuja, Ahmadu Bello University, Zaria and Sultan Qaboos University, Oman, for their support in this research

References

[1] *Handbook of Clay Science*, 2nd ed., Elsevier Ltd.,

Amsterdam, Nederland, 2013, pp. 118–1295.

[2] J. C. Hughes, R. J. Gilkes, and R. D. Hart, "Intercalation of reference and soil kaolins in relation to physico-chemical and structural properties," *Applied Clay Science*, vol. 45, pp. 24–35, 2009.

[3] J. C. Miranda-Trevino and C. A. Coles, "Kaolinite properties, structure and influence of metal retention on pH," *Applied Clay Science*, vol. 23, pp. 133–139, 2003.

[4] N. J. Saikia, D. J. Bharali, P. Sengupta, D. Bordoloi, R. L. Goswamee, P. C. Saikia, and P. C. Borthakur, "Characterization, beneficiation and utilization of a kaolinite clay from Assam, India," *Applied Clay Science*, vol. 24, pp. 93–103, 2003.

[5] S. K. Hubadillah, Z. Haruna, M. H. D. Othman, A. F. Ismail, and P. Gani, "Effect of kaolin particle size and loading on the characteristics of kaolin ceramic support prepared via phase inversion technique" *Journal of Asian Ceramic Societies*, vol. 4, pp. 164–177, 2016.

[6] M. Bellotto, A. Gualtieri, G. Artioli, and S. M. Clark, "Kinetic study of the kaolinite-mullite reaction sequence, Part I: Kaolinite dehydroxylation," *Physics and Chemistry of Minerals*, vol. 22 pp. 207–214, 1995.

[7] L. C. Edomwonyi-Otu, B. O. Aderemi, A. S. Ahmed, N. J. Coville, and M. Maaza, "Influence of thermal treatment on kankara kaolinite," *Opticon*, vol. 15, pp. 51–55, 2013.

[8] C. Belver, M. A. Banares, and M. A. Vicente, "Chemical activation of a kaolinite under acid and alkaline conditions," *Chemistry of Materials*, vol. 14 pp. 501–506, 2002.

[9] M. I. Khan, H. U . Khan, K. Azizli, S. Sufian, Z. Man, A. A. Siyal, N. Muhammad, and M. F. Rehman, "The pyrolysis kinetics of the conversion of Malaysian kaolin to metakaolin," *Applied Clay Science*, vol. 146, pp. 152–161, 2017.

[10] T. P. Dang, B. Chen, and D. Lee, "Application of kaolin-based catalysts in biodiesel production via transesterification of vegetable oils in excess methanol," *Bioresource Technology*, vol. 145, pp. 175–181, 2013.

[11] A. Y. Atta, B. Y. Jibril, B. O. Aderemi, and S. S. Adefila, "Preparation of analcime from local kaolin and rice husk ash," *Applied Clay Science*, vol. 61 pp. 8–13, 2012.

[12] N. Yang, Z. Zhang, N. Ma, H. Liu, X. Zhan, B. Li, W. Gao, F. Tsai, T. Jiang, C. Chang, T. Chiang, and D. Shi, "Effect of surface modified kaolin on properties of polypropylene grafted maleic anhydride," *Results in Physics*, vol. 7, pp. 969–974, 2017.

[13] S. M. A. El-Gamal, M. S. Amin, and M. Ramadan, "Hydration characteristics and compressive strength of hardened cement pastes containing nano-metakaolin," *Housing and Building National Research Center Journal*, vol. 13, pp. 114–121, 2017.

[14] G. A. Panagiotis and K. G. Kolovos, "Data on the physical and mechanical properties of soilcrete materials modified with metakaolin," *Data in Brief*, vol. 13, pp. 487–497, 2017.

[15] R. Siddique and J. Klaus, "Influence of metakaolin on the properties of mortar and concrete: A review," *Applied Clay Science*, vol. 43, pp. 392–400, 2009.

[16] A. M. Rashad, "Metakaolin as cementitious material: History, sources, production and composition–A comprehensive overview," *Construction and Building Materials*, vol. 41, pp. 303–318, 2013.

[17] M. R. Wang, D. C. Jia, P. G. He, and Y. Zhou, "Influence of calcination temperature of kaolin on the structure and properties of final geopolymer," *Materials Letters*, vol. 64, pp. 2551–2554, 2010.

[18] Q. Wan, F. Rao, S. Song, D. F. Cholico-Gonzalez, and N. L. Ortiz, "Combination formation in the reinforcement of metakaolin geopolymers with quartz sand," *Cement and Concrete Composites*, vol. 80, pp. 115–122, 2017.

[19] H. Wang, C. Li, Z. Peng, and S. Zhang, "Characterization and thermal behavior of kaolin," *Journal of Thermal Analysis and Calorimetry*, vol. 105, no. 1, pp. 157–160, 2011.

[20] S. Chandrasekhar, P. Raghavan, G. Sebastian, and A. D. Damodaran, "Brightness improvement studies on 'kaolin based' zeolite," *Applied Clay Science*, vol. 12, no. 3, pp. 221–231, 1997.

[21] H. Rahier, J. Wastiels, M. Biesemans, R. Willlem, A. G. Van, and M. B. Van, "Reaction mechanism, kinetics and high temperature transformations of geopolymers," *Journal of Material Science*, vol. 42, pp. 2982–2996, 2007.

[22] Z. Zhang, H. Wang, X. Yao, and Y. Zhu, "Effects of halloysite in kaolin on the formation and properties of geopolymers," *Cement and Concrete Composites*, vol. 34, pp. 709–715, 2012.

[23] A. Shvarzman, K. Kovler, G. S. Grader, and G. E. Shter, "The effect of dehydroxylation/ amorphization degree on pozzolanic activity of kaolinite," *Cement and Concrete Research*, vol. 33, pp. 405–416, 2003.

[24] B. Fabbri, S. Gualtieri, and C. Leonardi, "Modifications induced by the thermal treatment of kaolin and determination of reactivity of metakaolin," *Applied Clay Science*, vol. 73, pp. 2–10, 2013.

[25] B. R. Ilic, A. A. Mitrovic, and L. R. Milicic, "Thermal treatment of kaolin clay to obtain metakaolin," *Hemijska Industrija*, vol. 64, pp. 4, pp. 351–356, 2010.

[26] N. Salahudeen, A. S. Ahmed, C. S. Ajinomoh, and H. Hamza, "Surface area enhancement of pindiga bentonitic clay for usage as catalyst support," *Petroleum Technology Development Journal*, vol. 2, no. 2, pp. 65–73, 2012.

[27] A.S. Ahmed, N. Salahudeen, C. S. Ajinomoh, H. Hamza, and A. Ohikere, "Studies on mineral and chemical characteristics of pindiga bentonitic clay," *Petroleum Technology Development Journal*, vol. 2, no. 1, pp. 55–62, 2012.

[28] T. Hatakeyama and F. X. Quinn, *Thermal Analysis Fundamentals and Applications to Polymer Science*, 2nd ed. New York: John Wiley & Sons, Ltd, 1999.

[29] R. J. Konwar and M. De, "Effects of synthesis parameters on zeolite templated carbon for hydrogen storage application," *Microporous and Mesoporous Materials*, vol. 175, pp. 16–24, 2013.

[30] P.-Yuan Chen, *Tables of Key Lines in X–ray Powder Diffraction Patterns of Minerals in Clays and associated Rocks*. Bloomington, Indiana: The state of Indiana, 1977.

[31] A. O. Ajayi, A. Y. Atta, B. O. Aderemi, and S. S. Adefila, "Novel method of metakaolin dealumination - preliminary investigation," *Journal of Applied Sciences Research*, vol. 6, no. 10, pp. 1539–1546, 2010.

[32] A. K. Panda, B. G. Mishra, D. K. Mishra, and R. K. Singh, "Effect of sulphuric acid treatment on the physico-chemical characteristics of kaolin clay," *Colloids and Surfaces A: Physicochemical and Engineering Aspects*, vol. 363, pp. 98–104, 2010.

[33] R. Babalola, J. A. Omoleye, S. S. Adefila, F. K. Hymore, and O. A. Ajayi, "Comparative analysis of zeolite Y from Nigerian clay and standard grade," in *Proceeding International Conference on African Development Issues*, 2015, pp. 179–182.

[34] M. E. Awad, A. López-Galindo, M. M. El-Rahmany, H. M. El-Desoky, and C. Viseras, "Characterization of egyptian kaolins for health-care uses," *Applied Clay Science*, vol. 135, pp. 176–189, 2017.

[35] J. Aderiye "Characterisation of the Nigerian Kankara kaolinite clay particulates for automobile friction lining material development," *Chemical and Process Engineering Research*, vol. 29, pp. 24–33, 2014.

[36] S. A. Abo-El-Enein, M. Heikal, M. S. Amin, and H. H. Negm, "Reactivity of dealuminated kaolin and burnt kaolin using cement kiln dust or hydrated lime as activators," *Construction and Building Materials*, vol. 47, pp. 1451–1460, 2013.

[37] W. D. Keller, "Flint-clay facies illustrated within one deposit of refractory clay," *Clays and Clay Minerals*, vol. 26, pp. 237–243, 1978.

[38] W. D. Keller and R. P. Stevens, "Physical arrangement of high-alumina clay types in a Missouri clay deposit and implications for their genesis," *Clays and Clay Minerals*, vol. 31, pp. 422–434, 1983.

[39] G. Lombardi, J. D. Russell, and W. D. Keller, "Compositional and structural variations in the size fractions of a sedimentary and a hydrothermal kaolin," *Clays and Clay Minerals*, vol. 35, pp. 321–335, 1987.

[40] B. Lanson, D. Beaufort, G. Berger, A. Bauer, A. Cassagnabere, and A. Meunier, "Authigenic kaolin and illitic minerals during burial diagenesis of sandstones: A review," *Clays and Clay Minerals*, vol. 37, pp. 1–22, 2002.

[41] M. P. Krekeler, "Improved constraints on sedimentary environments of palygorskite deposits of the Hawthorne formation, Southern Georgia, from a detailed study of a core," *Clays and Clay Minerals*, vol. 52, pp. 253–262, 2004.

[42] C. Ma and R. A. Eggleton, "Surface layer types of

kaolinite: A high resolution transmission electron microscope study," *Clays and Clay Minerals*, vol. 47, pp. 181–191, 1999.

[43] K. Piyapaka, S. Tungkamani, and M. Phongaksorn, "Effect of strong metal support interactions of supported Ni and Ni-Co catalyst on metal dispersion and catalytic activity toward dry methane reforming reaction," *International Journal of Applied Science and Technology*, vol. 9, no. 4, pp. 255–259, 2016.